Development of predictive models for the probabilistic moisture risk assessment of internal wall insulation

Valentina Marincioni[a,*], Giampiero Marra[b], Hector Altamirano-Medina[a]

[a] Institute for Environmental Design and Engineering, University College London, 14 Upper Woburn Place, London WC1H 0NN, UK
[b] Department of Statistical Science, University College London, Gower Street, London WC1E 6BT, UK

A B S T R A C T

Solid wall buildings account for a quarter of the UK building stock and need to be thermally upgraded to meet national greenhouse gas emission targets. Internal wall insulation (IWI) is often the only option for the retrofit of solid walls, especially when they are of architectural or historical interest. However, IWI can lead to moisture accumulation within the existing wall, affecting the structural integrity of the building and the health of occupants. To avoid these issues, a thorough risk assessment is necessary.

This paper presents a method for developing predictive meta-models that can be used for a fast probabilistic moisture risk assessment of IWI, considering both the uncertainty and variability of input variables. First, in a Monte Carlo analysis, the uncertainty and variability of inputs were propagated through hygrothermal simulations. Then, generalised additive models for location, scale and shape (GAMLSS) were used to describe the relationship between inputs and response variables of the Monte Carlo analysis. The key input variables were identified by a global sensitivity analysis - using the elementary effects method - and in model building. Two types of response variable were considered for the models: variables based on percentage values (e.g. maximum relative humidity) and dose-response relationships (e.g. mould index). The paper shows that both risk assessment models had a good predictive power, highlighting the suitability of the developed method for the moisture risk assessment of the internal insulation of solid walls.

1. Introduction

The impact of greenhouse gas (GHG) emissions on climate change is of global concern; with the Paris Agreement, various countries agreed to reduce GHG emissions in the first legally binding global climate deal. In the UK, through the Climate Change Act, the Government has committed to the reduction of GHG emissions by at least 80% by 2050 (from 1990 levels). In order to help meet the target, the energy efficiency of existing buildings must be improved [1]. In the UK, solid wall buildings account for around 20% of the housing stock. Energy efficiency interventions on solid walls are less cost-effective than other measures commonly installed in the UK; for this reason, properties with solid walls are categorised as "hard-to-treat" [2]. As of December 2016, only 8% of UK's solid wall dwellings have been insulated [3]; this figure reflects the challenges of solid wall insulation but also highlights the potential of this intervention in contributing to the reduction of greenhouse gas emissions pledged by the UK Government. Internal wall insulation is one of the few solutions for the energy efficiency of solid walls, especially if the façade is of special architectural or historic interest. However, it can lead to moisture accumulation, which can be

detrimental to the health of occupants and the structural integrity of a building. A moisture risk assessment aims at evaluating the likelihood of building failures due to excessive moisture accumulation; it supports decision making and allows designers to choose suitable insulation systems based on information about the risk related to moisture.

2. Literature review

2.1. Moisture transfer in internally insulated walls

A suitable risk assessment must consider the relevant heat and moisture transfer mechanisms that might lead to moisture risk in internally insulated walls. The main moisture transfer mechanisms occurring in internally insulated solid walls are:

- capillary suction
- vapour diffusion
- solar-driven vapour diffusion.

Capillary suction can occur when open-porous materials are in

contact with liquid water. Wind-driven rain can be absorbed by bricks via capillary suction, having a considerable impact on the hygrothermal performance of solid brick walls [4]. Also, groundwater can rise through walls via capillary suction [5]. Capillary suction is contributing to moisture accumulation within solid walls, in liquid phase, but also allows redistribution of water in the wall, which can lower the moisture risk [6].

Water vapour diffusion is driven by gradients of vapour pressure. Vapour diffusion occurring from the indoor environment to the wall-insulation interface can contribute to moisture accumulation.

Solar-driven vapour diffusion [7] occurs when a solid wall is exposed to solar radiation and liquid water is present in the wall; water evaporates and diffuses towards areas of lower vapour pressure. Solar-driven vapour diffusion can be observed in solid walls in the UK, especially in walls with dark, porous surfaces exposed to direct solar radiation [8,9]. Solar-driven vapour diffusion can contribute to drying; however, moisture can accumulate in constructions with vapour tight interior finishes [10].

2.2. Moisture risk assessment methods

A number of methods for moisture risk assessment exist. The most common method for moisture risk assessment for internal wall insulation involves calculating the heat and moisture balance in building components. The heat and moisture balance is calculated through hygrothermal simulation software validated according to EN 15026:2007 [11], which consider the relevant phenomena in case of internal wall insulation, such as capillary suction and solar-driven vapour diffusion.

The moisture risk assessment of internal wall insulation is often performed through parametric studies, using deterministic hygrothermal simulations that consider either average [12–14] or worst-case [15–17] scenarios. A common worst-case scenario considers worst-case orientation (e.g. selecting the prevailing wind direction to account for worst-case wind-driven rain penetration) or worst-case occupancy levels (e.g. considering high occupancy to account for worst-case vapour diffusion). Sometimes, the severity of the scenario is itself a parameter of the study (e.g. occupancy level [18].)

Another approach considers the introduction of a safety margin for the risk assessment; an additional 1% of wind-driven rain was introduced within the wall structure to analyse unwanted rainwater penetration [19]. Although developed to assess risk related to poorly-installed external water-tight membranes in timber frame walls, this approach was then extended to other structures [20] and applied to the assessment of internal wall insulation [21].

However, the uncertainty and variability of inputs (e.g. the temporal variability of climate and the variability of hygric properties for traditional bricks) are not fully considered in the analysis, which can lead to an underestimation of risk. On the other hand, a probabilistic risk assessment can consider the influence of the uncertainty and variability of inputs on the risk estimate.

Probabilistic risk assessment provides estimates of the range and likelihood of a hazard or risk, rather than a single point estimate, and can be used to support risk management and decision making by assessing the impact of uncertainties on each of the potential options [22].

A common method of probabilistic risk assessment is to use the Monte Carlo analysis, which allows to propagate the uncertainty and variability of the inputs through available deterministic models, such as hygrothermal simulation models. Once the model and input distributions are specified, the Monte Carlo analysis allows for the estimation of the model output by generating input data from random sampling of the specified input distributions and performing deterministic simulations using the generated inputs [23]. The output of this analysis is then compared with failure criteria, in a process called risk evaluation.

The Monte Carlo analysis has been widely used for the probabilistic moisture risk assessment of internally insulated walls. These examples

of Monte Carlo-based moisture risk assessment considered the influence of the uncertainty and variability of various inputs on the moisture risk [6,24–26]. The outputs obtained from the Monte Carlo analysis were the distributions of mould index [24,25], number of hours above 80% and 95% relative humidity and freeze-thaw cycles [6,26]; these outputs were then compared with suitable failure criteria. Another Monte Carlo-based moisture risk assessment considered the uncertainty of mould growth models, as well as providing a stochastic representation of the external climate [27].

Furthermore, a risk management framework based on the Monte Carlo analysis was developed within the IEA Annex 55 on "Reliability of Energy Efficient Building Retrofitting - Probability Assessment of Performance and Cost" [28]. Finally, a probabilistic approach to moisture risk assessment was included in a conceptual reliability model for mould safety in buildings [29].

The use of a Monte Carlo-based probabilistic risk assessment has proven to be beneficial in assessing moisture risk taking into account the uncertainty and variability of inputs. However, one of its disadvantages is the time required for the risk assessment. This can be resolved with the development of meta-models.

Meta-models were developed within the IEA Annex 55 framework for the risk assessment of energy efficient retrofit [30,31] and applied to building energy simulations.

The aim of the current research is to develop statistical meta-models for the reduction of computational time in moisture risk assessment. In this paper, a statistical meta-model was built to describe the relationship between input variables and a response variable calculated through hygrothermal simulations, considering the case of internal wall insulation. For the development of the meta-model, additional information on the input variables affecting the response variable the most was required. This additional data was obtained through sensitivity analysis, which has been used extensively to inform modelling in building physics [32].

3. Methodology

The steps to develop a predictive model for probabilistic risk assessment include a Monte Carlo analysis, followed by a sensitivity analysis and the development of a statistical meta-model. In the first step, response variables related to moisture accumulation (e.g. maximum relative humidity) were obtained from the Monte Carlo analysis; the analysis considered the uncertainty and variability of the input variables, which include the hygrothermal properties of building materials, the internal climate and the weather. The Monte Carlo analysis consists of defining the probability density functions of input variables, generating random samples from inputs distributions, performing a deterministic simulation using the sampled inputs and aggregating the results into one or more response variables.

The sensitivity analysis provides relevant information on the relative importance of input variables on each response variable. Within the scope of this paper, the sensitivity analysis allowed us to identify some non-influential variables and reduce the number of variables for the development of a meta-model.

The meta-model was developed to reduce the computational time of numerical analyses; statistical models often require a reduced set of input variables and therefore can benefit from the results of a sensitivity analysis.

The steps required for the Monte Carlo analysis, the sensitivity analysis and the development of the meta-model are explained in detail in this paper, through the application of the procedure to an internally insulated solid brick wall.

3.1. The case study - internally insulated wall

The cross-section of a solid brick wall with capillary active internal insulation was analysed. The wall is formed by a layer of solid brick, a
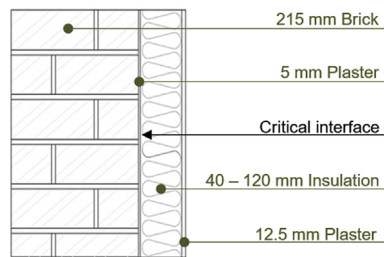
Fig. 1. Case study wall cross-section.

Table 1

Material functions and related material parameters (from Zhao et al. [35]).

Material function	Symbol	Units	Material parameters
Moisture retention function	$\theta(pC)$	$m^3 m^{-3}$	θ_{eff}
Water vapour permeability	$k_v(\theta)$	s	θ_{por}, μ
Liquid water conductivity	$k_l(\theta)$	s	θ_{eff}, $k_{l,eff}$
Thermal conductivity	$\lambda(\theta)$	$W m^{-1} K^{-1}$	θ_{eff}

layer of plaster acting as a bonding coat, a layer of woodfibre insulation and a second layer of plaster (outside to inside, see Fig. 1). In the first layer, the wall is solely composed by solid brick; this can be a valid assumption for a simplified analysis, as mortar has been found to have a small impact on the hygrothermal behaviour of internally insulated solid brick walls under realistic climate conditions [33]. Therefore, for the purpose of the analysis, the simulation of the combined heat and moisture transfer was simplified to one-dimensional, following the horizontal axis of the wall. However, the same approach can be extended to two- or three-dimensional simulations.

The proposed probabilistic risk assessment considers the possible variations of design parameters, which could change through interventions, and the uncertainty and variability of other parameters. In the solid wall, the water vapour diffusion resistance of insulation was treated as a design variable, while other hygrothermal properties of insulation and the properties of brick and plaster were considered non-design parameters.

The insulation thickness was treated as a design variable; the range used for the insulation thickness (i.e. 40 mm–120 mm) represents the thickness of woodfibre boards available in the market. A thickness of 215 mm was considered for the brick in the analysis, since it has been estimated that 70% of solid wall buildings in England have that thickness [34]. The thickness used for the first and second layers of the plaster was 5 mm and 12.5 mm respectively, according to building practice.

The risk assessment considered the temporal variability of external climate (i.e. using several years of climate data), and the spatio-temporal variability of surface coefficients (i.e. considering the full range of coefficients); the rain exposure coefficient was treated as design parameter. The indoor environment and internal surface coefficients were not treated as design parameters, but their uncertainty and variability were considered.

The probabilistic risk assessment considered risks related to moisture accumulation, which can occur at the critical interface between the existing wall and the applied insulation system. Various failure criteria can be used for the assessment, with the aim of avoiding condensation, mould growth, wood rot and other issues.

3.2. Monte Carlo analysis

3.2.1. Input variables

A Monte Carlo analysis starts with the selection of probability density functions for the input variables; in this paper, the distributions were derived from literature and material databases.

Material parameters for bricks were taken from the relevant academic literature [35,36], whereas the parameters for insulation and plaster are from the material database of Delphin [37], the hygrothermal simulation software used for the analysis. For a good characterization of building materials, it is advised to describe some hygrothermal properties as functions of other parameters (e.g. moisture content and capillary pressure). These functions are affected by various material parameters, as described by Zhao et al. [35] and shown in Table 1.

In this paper, it was assumed that the hygric functions can be

described by the product of these material parameters and fixed relative functions, which represent a type of brick, insulation or plaster. Therefore, the sampling of hygric material properties will only consider the material parameters identified.

The hygrothermal material parameters are described in Table 2. The probability density functions describe types - or clusters - of materials, as opposed to specific or general materials. In particular, the brick type described is a historic brick made of clay, loam and sand [36]; woodfibre insulation and lime plaster were, respectively, the type of insulation and plaster considered. The analysis considered the possibility of having an insulation system with additional vapour resistance; this has been implemented in the analysis having the vapour diffusion resistance coefficient μ_i of a wider range than typical woodfibre insulation.

Material properties of open-porous materials depend on the porous structure of materials; therefore, in materials such as brick, stone and plaster, there can be associations between material properties (e.g. open porosity and density [38]). A rank correlation matrix of material parameters of bricks [35] was integrated in the probabilistic risk assessment through the Iman and Conover method [39], which is a rank transformation commonly used to consider associations between variables in a model [40,41].

In order to characterise the climate variability, a collection of 22 years of weather data was considered in the analysis, as the existing typical and near-extreme reference years do not necessarily represent typical and near-extreme climates in relation to moisture risk [42].

For the development of the meta-model, all orientations were considered in the sensitivity analysis and model-building; therefore the orientation was a uniform variable from 0° to 360°. The same applies to the surface absorptivity of short-wave (solar) radiation, which is determined by the colour of the external wall, and it is made to vary in its whole range. During the moisture risk assessment, these values can be set to describe the case under analysis, as shown in Section 4.4.

External surface parameters such as convective heat transfer coefficient, ground emissivity of long-wave radiation and surface absorptivity of short-wave radiation were taken from literature, as shown in Table 3. For both the Monte Carlo and sensitivity analyses, the whole range was considered for each parameter.

For the internal climate, temperature and vapour pressure excess were determined. The internal temperature was kept constant at 20 °C. The internal vapour pressure excess considered in the analysis was derived from the results of the Warm Front research project [46]. The research identified vapour pressure excess in UK living rooms and bedrooms for dwellings in fuel poverty (values normalized at an external temperature of 5 °C).

Random samples of vapour pressure excess at 5 °C were extracted from the vapour pressure excess distribution in UK bedrooms. The time series for the vapour pressure was given by the interpolation of the sampled value at different external temperatures, using the function in BS EN ISO 13788 [47]. The resulting internal vapour pressure was given by the sum of external vapour pressure and internal vapour pressure excess.

Internal surface parameters were taken from literature, as shown in Table 4.

Table 2
Material parameters and probability density functions for hygrothermal simulations. A: first probability distribution parameter (i.e. mean for normal distribution, minimum for uniform distribution), b: second probability distribution parameter (i.e. standard deviation for normal distribution, maximum for uniform distribution).

No.	Input Variable	Symbol [Units]	Distribution	a	b
1	Brick density	$\rho_b\,[kgm^{-3}]$	Normal	1730.0	108.5
2	Brick specific heat capacity	$c_{e,b}\,[Jkg^{-1}K^{-1}]$	Normal	874.41	63.05
3	Brick thermal conductivity	$\lambda_b\,[Wm^{-1}K^{-1}]$	Normal	0.497	0.102
4	Brick open porosity	$\theta_{por,b}\,[m^3m^{-3}]$	Normal	0.347	0.041
5	Brick effective saturation moisture content	$\theta_{eff,b}\,[m^3m^{-3}]$	Normal	0.314	0.0034
6	Brick water vapour resistance factor	$\mu_b\,[-]$	Normal	13.5	2.4
8	Brick liquid water conductivity at effective saturation	$k_{l,eff,b}\,[s]$	Uniform	1.2E-9	2.4E-8
9	Insulation density	$\rho_i\,[kgm^{-3}]$	Uniform	120	300
10	Insulation specific heat capacity	$c_{e,i}\,[Jkg^{-1}K^{-1}]$	Uniform	1000	2100
11	Insulation thermal conductivity	$\lambda_i\,[Wm^{-1}K^{-1}]$	Uniform	0.039	0.063
12	Insulation open porosity	$\theta_{por,i}\,[m^3m^{-3}]$	Uniform	0.40	0.99
13	Insulation effective saturation moisture content	$\theta_{eff,i}\,[m^3m^{-3}]$	Uniform	0.30	0.89
14	Insulation water vapour resistance factor	$\mu_i\,[-]$	Uniform	3	225
15	Insulation liquid water conductivity at effective saturation	$k_{l,eff,i}\,[s]$	Uniform	4.9E-9	2.2E-8
16	Plaster density	$\rho_p\,[kgm^{-3}]$	Uniform	1240	1800
17	Plaster specific heat capacity	$c_{e,p}\,[Jkg^{-1}K^{-1}]$	Uniform	800	1100
18	Plaster thermal conductivity	$\lambda_p\,[Wm^{-1}K^{-1}]$	Uniform	0.28	0.82
19	Plaster open porosity	$\theta_{por,p}\,[m^3m^{-3}]$	Uniform	0.30	0.53
20	Plaster effective saturation moisture content	$\theta_{eff,p}\,[m^3m^{-3}]$	Uniform	0.28	0.46
21	Plaster water vapour resistance factor	$\mu_p\,[-]$	Uniform	8	51
22	Plaster liquid water conductivity at effective saturation	$k_{l,eff,p}\,[s]$	Uniform	8.7E-12	3.0E-9
34	Insulation thickness	$x_i\,[m]$	Uniform	0.04	0.12

3.2.2. Monte Carlo analysis: sampling

The replicated Latin Hypercube Sampling was used for the sampling stage of the Monte Carlo analysis. Compared with the simple random Monte Carlo sampling, the Latin Hypercube Sampling is a stratified sampling method which is able to reduce the size of the necessary sample while accurately depicting the probability density function of the input random variables.

Variations of the standard Latin Hypercube sampling were used in this paper, with the aims of improving the efficiency of the sampling, implementing a stopping criterion and considering correlated variables. First, the Latin Hypercube Sampling was optimised according to the maximin space-filling criterion, which maximises the minimum distance between any two points.

Twenty mini Latin Hypercubes of sample size 100 were generated (as opposed to one full Latin Hypercube of size 2000) to allow for a stopping criterion for the Monte Carlo analysis [49]. Finally, The Iman and Conover method of imposing rank correlations on pairs of input factors was implemented in the sampling stage, as described by Zhao [40].

Dynamic equilibrium in the simulation was ensured by performing the simulation for various years until the last two years have a negligible difference (assumed as lower than the accuracy of a relative humidity sensor, $\varepsilon(\phi) = \pm 2.5\%$). For this application, two years are required. The simulations started in October, to consider complete wetting and drying cycles.

Table 4
Internal parameters and probability density functions for hygrothermal simulations.

No.	Input Variable	Symbol [Units]	Distribution	a	b	Ref.
25	Internal vapour pressure excess (bedroom)	$\Delta p_v\,[Pa]$	Normal	325.421	137.131	[46]
26	Combined heat transfer coefficient, internal	$h_i\,[Wm^{-2}K^{-1}]$	Uniform	3	15	[48]
27	Vapour transfer coefficient, internal	$v_i\,[sm^{-1}]$	Uniform	0.1E-7	1E-7	[48]

3.2.3. Monte Carlo analysis: response variables

The input variables, described in Section 3.2.1 and sampled according to Section 3.2.2, were used in deterministic simulations using the hygrothermal simulation software Delphin. The results were aggregated into response variables, which were selected according to the failure criteria used in the risk assessment. More than one response variable can be used for the assessment of moisture risk in internally insulated walls. For example, with fully bonded woodfibre insulation systems, the maximum relative humidity (in a year) at the wall-insulation interface can be used to evaluate condensation risk [50] and

Table 3
External parameters and probability density functions for hygrothermal simulations.

No.	Input Variable	Symbol [Units]	Distribution	a	b	Ref.
24	External climate	Cli	Discrete Uniform	22		[42,43]
23	Orientation	$\gamma\,[°]$	Uniform	0	360	
28	Convective heat transfer coefficient, external	$h_{c,e}\,[Wm^{-2}K^{-1}]$	Uniform	12.5	50	[44]
30	Short wave radiation - absorption coefficient	$\alpha_{sw}\,[-]$	Uniform	0.5	0.9	
31	Short wave radiation - ground reflectivity (albedo)	$A\,[-]$	Uniform	0.05	0.56	[45]
32	Long wave radiation - ground emissivity	$\varepsilon_g\,[-]$	Uniform	0.86	0.97	[45]
33	Rain exposure coefficient	$k_{rain}\,[-]$	Uniform	0	1	

the maximum moisture content of woodfibre (in mass percent) can be used to evaluate wood rot risk [51]; these criteria are based on percentage values. Other failure criteria used in moisture risk assessment are more complex than the percentage-based criteria just described. If there is risk of mould growth then this can be evaluated through dose-response relationships and the related response variables (e.g. mould index [52] or relative dose [53]). These variables derive from models that describe mould growth as a function of substrate category and different levels of exposure to certain environmental conditions.

In this work, both response variables based on percentage values and those based on dose-response relationships were considered for the development of predictive models for probabilistic moisture risk assessment.

3.3. Sensitivity analysis

A sensitivity analysis was carried out to identify both the input variables that have the highest effect on the output and those that do not considerably affect the output and hence can be ignored, which is useful as statistical models require a parsimonious set of variables.

The sensitivity analysis was carried out through scatter plots and the elementary effects method. Scatter plots present each input variable against the response variable; they help identifying relationships between variables by looking at the shape of the plot. However, they have limited exploratory power when the input variables are related with each other.

The elementary effects method is a model-independent screening method, which provides a qualitative analysis of the input variables that affect the response variable the most [54]. The method considers the variation of one input variable at a time while the other variables are fixed at a random value. This process is repeated N times, with a different set of fixed values at each iteration; the fixed values are obtained through a random sampling. This is a global sensitivity analysis method, which considers interaction effects of input variables and non-monotonic relationships.

In this paper, a radial design was implemented for $N = 20$ iterations. For each iteration, the elementary effect related to one input variable is the difference between the response variable Y considering the variation of the one input variable and the response variable considering the baseline terms, divided by the sampling step for the radial design. The sampled value x_i of one input variable was uniformly distributed in the interval [0,1]; at a later stage these values were converted into input variables, and inverse cumulative distribution functions were used to transform sampled values into non-uniformly distributed inputs. For the jth iteration and the ith input variable, the elementary effect was computed as:

$$EE_i^j = \frac{Y(x_i^{(u)} x_i^{(u)}) - Y(x_i^{(v)} x_i^{(u)})}{x_i^{(u)} - x_i^{(v)}}$$

(1)

where u and v denote two rows of the radial sampling matrix for the jth iteration, with u containing the baseline terms and v the auxiliary terms of the radial design [55].

Latin Hypercube Sampling was used to obtain the random sampling matrix. The sensitivity measures μ, $\mu^\star$ and σ were extracted from the response variable, applying the following equations:

$$\mu_i = \frac{1}{N} \sum_{j=1}^{N} EE_i^j$$

(2)

$$\mu_i^\star = \frac{1}{N} \sum_{j=1}^{N} |EE_i^j|$$

(3)

$$\sigma_i^2 = \frac{1}{N-1} \sum_{j=1}^{N} (EE_i^j - \mu)^2$$

(4)

with EE_i^j the elementary effect of the ith variable in the jth screening path. The value $\mu^\star$ allows for the identification of the overall influence of an input variable on the response variable, considering non-monotonic relationships; the mean μ has the same purpose but does not consider non-monotonic relationships, which can be identified by the comparison of $\mu^\star$ and μ. Finally, σ considers interaction effects.

3.4. Predictive meta-models

A predictive model was created for each type of response variable; the models were built to describe the relationship between the input variables and the response. The data used were generated with the Monte Carlo analysis described in Sections 3.2.1 to 3.2.3.

The models were built using generalised additive models (GAM) [56] and generalised additive models for location scale and shape (GAMLSS), as introduced by Rigby and Stasinopoulos [57] and implemented by Marra and Radice [58]. The GAM and GAMLSS models were implemented using the gam() function from the mgcv R package and gamlss() from the GJRM R package [67,68]. Both models can deal with many types of inputs including categorical and continuous variables. The input variables for the model, described in 3.2.1, were considered continuous in most cases. The only variable which entered the model as categorical was the external climate.

The choice of appropriate model depends on the distribution of the response variable. Many relevant response variables were found for the moisture risk assessment of internal wall insulation, as mentioned in Section 3.2.3. They were divided into two groups: the variables based on percentage values (e.g. maximum relative humidity, moisture content) and the variables based on a dose-response relationship (e.g. mould index, dose). Maximum relative humidity was the response variable used in this paper to describe model building for percentage-based response variables; the mould index [59–61], considering kiln-dried spruce as substrate category, was the response variable used to describe model building in case of dose-response relationships.

3.4.1. Response variables and distributions

For the selected statistical methods, the first step consists of finding a distribution that fits the response variable. The goodness of fit of these distributions was assessed using Q-Q plots of normalized quantile residuals [57].

The response variables based on percentage values are continuous variables that vary from 0 to 1. In such cases, the beta distribution is an appropriate choice. It has the probability density function (pdf) $f(y) = \frac{y^{\alpha_1 - 1}(1-y)^{\alpha_2 - 1}}{B(\alpha_1, \alpha_2)}$ where $\alpha_1 = \frac{\mu(1-\sigma^2)}{\sigma^2}$, $\alpha_2 = \frac{(1-\mu)(1-\sigma^2)}{\sigma^2}$ and $B(\cdot,\cdot)$ is the beta function. The expectation of Y according to this distribution's parametrisation is $E(Y) = \mu$ whereas the variance is $V(Y) = \sigma^2 \mu(1-\mu)$. Both the mean μ and standard deviation σ need to fall within the interval [0, 1]. This is the distribution that was chosen to develop the predictive model for percentage-based response variables.

The response variables based on a dose-response relationship are either null or positive, because mould won't develop at all if the environmental conditions are below a critical value. Therefore, a two-part model was developed as a combination of a binary regression, to describe instances when the response variable is zero or not (binary variable), and a GAMLSS to describe the behaviour of the response variable for values higher than zero (continuous, positive variable). The binary part of the response variable is described by a Bernoulli distribution with probability mass function equal to p if $y = 1$ and $1 - p$ if $y = 0$. In this case, the expectation and variance are given by $E(Y) = p$ and $V(Y) = p(1-p)$. Parameter p describes the probability that the response is equal to 1 and must take values in the interval [0, 1]. The model used for the binary part was a binary regression implemented using the GAM method, which considers the Bernoulli distribution. Positive variables can be described by a gamma or a Weibull distribution. For example, the pdf of a Weibull distribution can be written as

$f(y) = \frac{\sigma}{\mu}\left(\frac{y}{\mu}\right)^{\sigma-1}\exp-\left(\frac{y}{\mu}\right)^{\sigma}$. Here, $E(Y) = \mu\Gamma\left(\frac{1}{\sigma}+1\right)$, $V(Y) = \mu^2\left[\Gamma\left(\frac{2}{\sigma}+1\right)-\left(\Gamma\left(\frac{1}{\sigma}+1\right)\right)^2\right]$, $\Gamma(\cdot,\cdot)$ is the gamma function, and μ and σ have to be positive.

3.4.2. Link function

When building a model, the constraints on the parameters' spaces must be satisfied. In particular, every distribution is described by parameters that can be bounded. Link functions are used to ensure that the bounds of the distribution fitting the response variable are met [56].

Link functions that are commonly used for response variables that lie in the interval [0, 1] are the probit, logit and complementary log-log link functions. For positive response variables, a common link function is the log link, based on the natural logarithm.[1]

3.4.3. Input variables and splines

These statistical methods allowed us to account for the possible presence of non-linear effects of the input variables, or *covariates*. This was achieved by using smooth functions of continuous covariates (e.g. $s(x)$ where x is a generic covariate) that were represented using a penalised spline approach. The main idea behind this method is to let the data determine the shape of the effects that covariates have on the response of interest without making a priori assumptions [56]. Input variables are included in the meta-models by specifying the parameters of the distributions described above as functions of them.

3.4.4. Variable selection

Many input variables were considered for the Monte Carlo analysis. However, the predictive model needs to have a balance between parsimony and complexity; hence, starting with a full model of 34 variables was not ideal. The information from the sensitivity analysis was used to identify the input variables having limited influence on the response and the model-building started with an arbitrary full model of 16 variables.

Then, the variable selection was done during model-building. The most influential covariates in the models were chosen using backward selection, with the Akaike information criterion (AIC) and the Bayesian information criterion (BIC), as well as the statistical significance of the model terms (to favour more parsimonious models). Variables were discarded one by one and a new model fitted at each step; this process was repeated until the model fits worsened.

4. Probabilistic risk assessment

4.1. Monte Carlo analysis results

The response variables, maximum relative humidity and mould index, were obtained from the Monte Carlo analysis (see Fig. 2).

It is important to note that, while the mould index is typically in the interval [0,6], in this paper the upper limit for mould growth was removed to reveal the whole response distribution. As the removed function describes the mould behaviour for a mould index higher than 4 [62], the risk assessment can consider only the mould index in the interval [0,4]; nevertheless, this interval is satisfactory for the assessment of mould growth at interfaces [63].

4.2. Sensitivity analysis of input variables

Scatter plots were generated for all the input variables, plotting each variable against the response variables maximum relative humidity and mould index. Considering the scatter plots, only three input variables

---

[1] According to the notations in this paper, the inverse of the link function is applied to the right-hand side of the model equation. For example, an exponential function is applied when the log link is considered.

showed influence on the response variable: the effective moisture content of insulation, the rain exposure coefficient and the wall orientation. However, scatter plots do not consider association between input variables, therefore they could not reveal much in our case. A screening according to the elementary effects method was performed to help unveil input variables with limited influence on the response variable.

Tables 5 and 6 describe the ranking of input variables according to the response variables of maximum relative humidity and mould index, respectively. The ranking was performed according to the sensitivity measure μ^*. The other sensitivity variables were used to identify non-monotonic relationships and interaction effects.

The most important input variables for the maximum relative humidity were found to be the rain exposure coefficient k_{rain}, the vapour diffusion resistance coefficient of the insulation μ_i and the orientation γ. They are followed by the external climate Cli, the effective saturation moisture content of insulation $\theta_{eff,i}$ and the insulation thickness x_i. The sensitivity measure μ showed that orientation and climate have a non-monotonic relationship with the response variable. Finally, the sensitivity measure σ showed that the aforementioned variables and the vapour diffusion resistance coefficient present high interaction effects.

The porosity θ_{por}, specific heat capacity c_e and density ρ of materials do not have a considerable influence on the response variable. Little influence was found for the emissivity of the surrounding ground ε_g, the thermal conductivity of the plaster λ_p and the indoor vapour pressure excess Δp_v.

The design variables were among the inputs having the highest influence on the maximum relative humidity; for the development of the meta-model, these variables were made to vary in their whole possible range. From a building physics perspective, the sensitivity analysis shows that the selection of correct design options can influence the maximum relative humidity considerably. Of the non-design variables, the external climate had the greatest influence on the maximum relative humidity; the only way to reduce this influence is to protect the wall from the external climate (i.e. modifying the external surface parameters). With existing buildings, some parameters must be set to describe the wall assessed, such as the wall orientation and the short-wave absorption coefficient, associated with the surface colour. For model-building, these two parameters were made to vary in their whole range, so that the developed model can be used for the assessment of all 215 mm-thick brick walls in one location, considering all orientations and surface colours.

For the mould index, the orientation γ, the rain exposure coefficient k_{rain} and the effective saturation moisture content of insulation $\theta_{eff,i}$ were found to be the most important input variables, followed by the external climate Cli, the insulation liquid water conductivity $k_{l,eff,i}$, the insulation thickness x_i and the vapour diffusion resistance coefficient of the insulation μ_i. Again, orientation and climate have a non-monotonic relationship with the response variable. Finally, the sensitivity measure σ showed that the above mentioned variables have high interaction effects. The lowest ranked variables are consistent with the previous case.

Overall, the sensitivity analysis for the two response variables showed a fairly consistent ranking. Again, the ranking showed that design variables have the highest influence on the response variable; therefore, the selection of appropriate design interventions might have a considerable influence on the mould index. The ranking identified by the screening exercise was consistent with their importance from a building physics perspective. It was interesting to note that vapour pressure excess did not have a high impact on the response variable, being on the lower half of the ranking for both cases.

This information was used for building the predictive meta-model. Specifically, this made it possible to build models with input variables that are important from both the statistical and building physics points of view.

(a) Histogram of maximum relative humidity

(b) Histogram of mould index
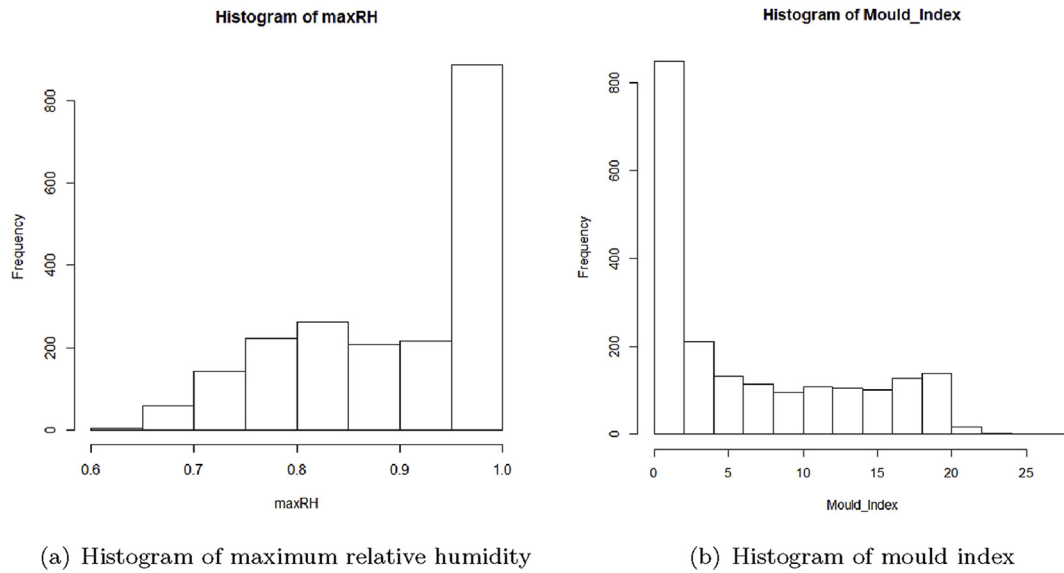
Fig. 2. Histograms of response variables.

Table 5
Elementary effects, considering maximum relative humidity as response variable.

μ^*	σ	μ	Variable symbol	No.
37.640	64.554	37.640	k_{rain}	33
28.060	123.153	28.060	μ_i	14
16.866	42.618	−3.017	γ	23
9.563	33.186	2.470	Cli	24
8.733	11.052	−8.730	$\theta_{eff,i}$	13
6.857	9.486	6.857	x_i	34
2.647	7.117	2.459	$k_{l,eff,b}$	8
1.835	2.972	−1.835	$k_{l,eff,i}$	15
1.619	2.763	−1.619	α_{sw}	30
1.117	4.401	1.092	λ_b	3
1.089	3.044	−0.127	μ_b	6
0.964	2.522	−0.400	$h_{c,e}$	28
0.957	2.939	−0.672	$\theta_{eff,p}$	20
0.912	1.341	−0.912	A	31
0.629	1.039	−0.629	λ_i	11
0.485	1.291	−0.230	$k_{l,eff,p}$	22
0.249	0.403	−0.249	h_i	26
0.128	0.278	0.097	$\theta_{eff,b}$	5
0.023	0.058	−0.021	v_i	27
0.023	0.055	−0.018	λ_p	18
0.021	0.051	−0.010	$c_{e,b}$	2
0.020	0.144	0.020	Δp_v	25
0.012	0.028	−0.011	ρ_b	1
0.012	0.034	0.010	ε_g	31
0.010	0.031	−0.002	ρ_i	9
0.006	0.018	0.004	ρ_p	16
0.006	0.018	0.003	$\theta_{por,i}$	12
0.006	0.013	0.004	$c_{e,i}$	10
0.004	0.013	−0.001	$c_{e,p}$	17
0.003	0.007	0.001	$\theta_{por,b}$	4

Table 6
Elementary effects, considering mould index as response variable.

μ^*	σ	μ	Variable symbol	No.
14.161	8.724	36.434	γ	23
13.14	13.14	20.881	k_{rain}	33
11.738	−11.738	19.95	$\theta_{eff,i}$	13
3.765	1.339	14.128	Cli	24
2.925	−2.925	7.589	$k_{l,eff,i}$	15
2.435	2.43	4.815	x_i	34
2.422	2.422	6.687	μ_i	14
1.371	−1.299	4.266	$\theta_{eff,p}$	20
1.155	−1.155	2.263	$h_{c,e}$	28
0.963	0.646	2.388	$k_{l,eff,b}$	8
0.757	−0.662	2.191	$k_{l,eff,p}$	22
0.412	−0.298	0.863	λ_b	3
0.269	0.269	0.527	μ_b	6
0.267	−0.165	0.602	α_{sw}	30
0.204	−0.108	0.447	A	31
0.15	0.046	0.352	λ_i	11
0.118	0.081	0.321	h_i	26
0.053	−0.019	0.137	$\theta_{eff,b}$	5
0.036	0.036	0.256	Δp_v	25
0.014	−0.003	0.048	λ_p	18
0.011	−0.01	0.029	$c_{e,b}$	2
0.008	−0.007	0.018	ρ_b	1
0.007	0.003	0.026	$\theta_{por,i}$	12
0.006	−0.002	0.019	v_i	27
0.006	0.003	0.026	ρ_i	9
0.004	0	0.013	$c_{e,p}$	17
0.003	0.002	0.012	$c_{e,i}$	10
0.003	−0.002	0.008	ε_g	31
0.003	0.002	0.008	ρ_p	16
0.002	0.001	0.008	$\theta_{por,b}$	4

4.3. The statistical meta-models

Two different meta-models were built considering different types of response variables. The first meta-model considers a response variable based on percentage values (here represented by the maximum relative humidity), and the second model considers a response based on a dose-response relationship (here represented by the mould index).

Maximum relative humidity takes values within the interval [0, 1]. According to the analysis of quantile residuals (see Fig. 3), the beta distribution was considered appropriate in this case.

Based on the ranking provided by the sensitivity analysis, the variable selection started with a full model of 16 covariates (i.e. following the ranking in Table 5). The final model (after variable selection) contains 10 covariates. Prediction was performed through transforming the model output according to the link function chosen for this case. In particular the cumulative logistic distribution function was employed (here called plogis), so that the values were all in the interval [0, 1]; this is the inverse of the logit link function. Given that the expectation for a beta distribution is equal to the mean, μ, the equation of
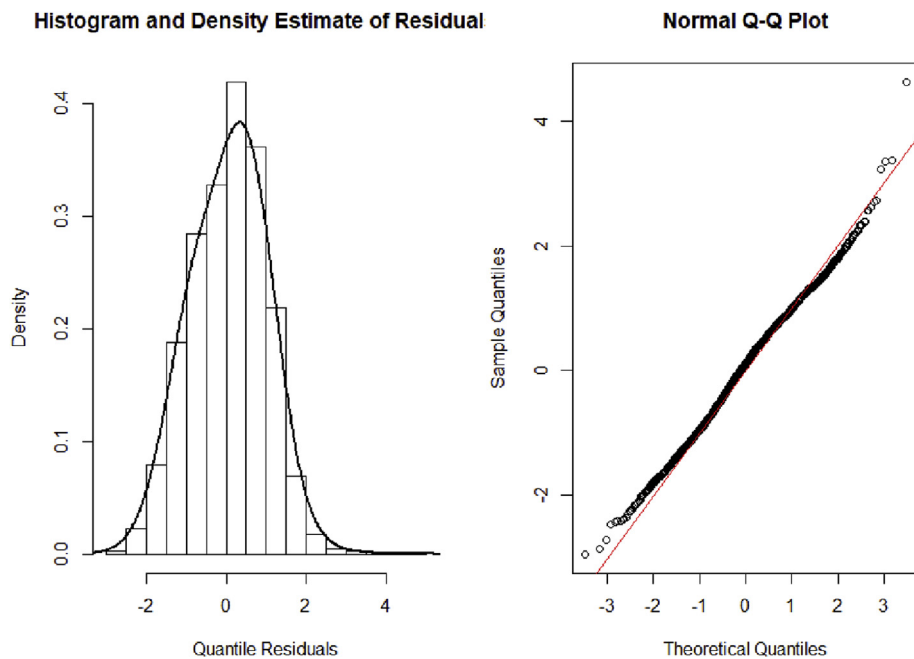
Fig. 3. Analysis of quantile residuals using the beta distribution, for the response variable maximum relative humidity.

interest is

$$\mu = plogis\{\alpha + s_1(\gamma) + s_2(Cli) + s_3(\theta_{eff,i}) + s_4(x_i) + s_5(k_{l,eff,b}) + s_6(k_{l,eff,i})$$
$$+ s_7(\alpha_{sw}) + s_8(\lambda_b) + s_9(k_{rain}) + s_{10}(\lambda_i)\}, \tag{5}$$

where smooth functions of continuous variables (implemented using cubic regression splines) were considered as well as a smoothed and parsimonious version of the categorical variable.

Fig. 4 shows the predicted values of maximum relative humidity (obtained with the developed model) against the real value of the response variable, which it is assumed to be the maximum relative humidity obtained with the Monte Carlo analysis and shown in Section 4.1. This plot shows the relationship between prediction and real value; the model captures the overall behaviour of the response variable if the predicted and real values are aligned.
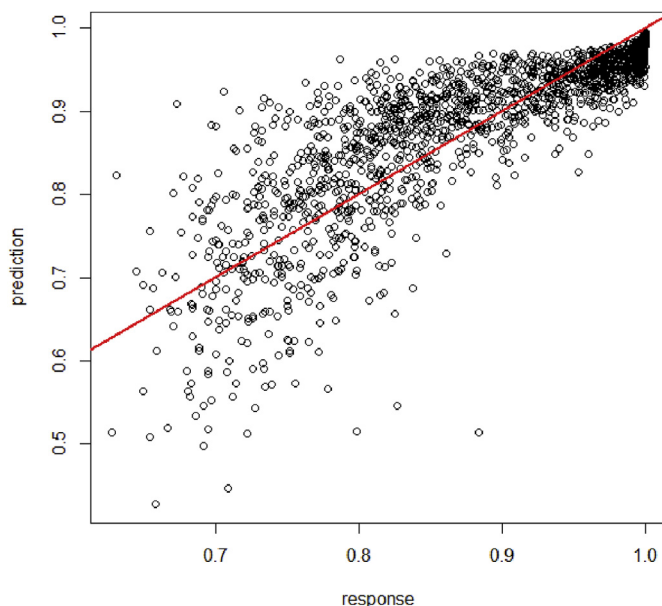

Fig. 4. Comparison of response variable and prediction, for the response variable maximum relative humidity.

The reference red line indicates the case in which the prediction would be the same as the response. The data-points are overall aligned with the red line, suggesting that the model can predict the mean values for the response reasonably well. In terms of variability, there was a high spread at lower values of maximum relative humidity and a lower spread at higher values. For the moisture risk assessment, the behaviour of relative humidity at high values is of more interest; for example, to avoid condensation, the maximum relative humidity must be below 95% [50]. At these values, variability is lower which makes the prediction task more precise.

The approach also allows other response variables, such as mean relative humidity or maximum moisture content, to be treated similarly.

A response variable based on a dose-response relationship has either null or positive values. In this case, if the exposure to favourable environmental conditions is insufficient for the development of mould, the mould index would be zero. When mould develops, the mould index would be a positive value; this value can be used to evaluate the extent of mould growth.

Therefore, the response variable was divided in a binary part and a continuous positive part. As a result, a two-part model was developed where the predicted values are given by the product of the predictions from the binary GAM and GAMLSS models. From a building physics perspective, the binary model describes the occurrence of mould growth, whereas the GAMLSS describes the extent of mould growth when it occurs.

Variables that determine the occurrence of mould growth might not be the same variables as the ones influencing the extent of mould growth. Therefore, the variable selection was done independently, although it started in both cases with a full model determined by the ranking identified through the sensitivity analysis. The backward selection approach was performed, starting with a full model of 16 variables.

The binary part of the response variable was described by a Bernoulli distribution, where the expectation is equal to the mean or probability p. For the binary model, the best link function identified for this data was the complementary log-log function, an asymmetric link function. The inverse of the link function for the expectation p is shown in equation (7). Regarding variable selection, the backward selection led to the following model, with 11 significant variables:

$$\eta = \alpha + s_1(\gamma) + s_2(\theta_{eff,i}) + s_3(Cli) + s_4(\mu_i) + s_5(k_{l,eff,b}) + s_6(x_i)$$
$$+ s_7(k_{l,eff,i}) + s_8(\lambda_b) + s_9(k_{rain}) + s_{10}(\alpha_{sw}) + s_{11}(\lambda_i), \tag{6}$$

$$p = 1 - \exp\{\exp(\eta)\} \tag{7}$$

For the GAMLSS model, the distribution that best fitted the response variable was the Weibull distribution. Using variable selection, the final model contains 12 covariates. Predictions were obtained using the log link function and a set of smooth functions of input variables. Given that the expectation of a Weibull distribution depends on both its parameters, the equations used were

$$\mu = \exp\{\alpha + s_1(\gamma) + s_2(\theta_{eff,i}) + s_3(Cli) + s_4(\mu_i) + s_5(k_{l,eff,b}) + s_6(x_i)$$
$$+ s_7(k_{l,eff,i}) + s_8(\theta_{eff,p}) + s_9(k_{l,eff,p}) + s_{10}(\mu_b) + s_{11}(k_{rain}) + s_{12}(\alpha_{sw})\}, \tag{8}$$

and

$$\sigma = \exp\{\alpha + s_1(\gamma) + s_2(\theta_{eff,i}) + s_3(Cli) + s_4(\mu_i) + s_5(k_{l,eff,b})\} \tag{9}$$

To ease the computational effort, the variables in equation (9) were selected via forward selection, based on the knowledge of the physical mechanisms that influence the variability of the response variable. Having obtained the individual models, the final prediction was given by the product of the prediction of the two models.

Fig. 5 shows the predicted values for the mould index, obtained with the two-part model, against the response variable obtained with the Monte Carlo analysis.

In the range of the response variable [5,18], the predicted values are slightly lower than the values of the response variable. This suggests an underestimation of the risk. On the other hand, there is an over-estimation when the response variable mould index is above 18. However, we are mainly interested in the occurrence of mould growth, described by the binary part of the model and in the range (0,3) of the continuous response variable; criteria for the avoidance of mould growth usually require the mould index at interfaces to be below 3 [63], which corresponds to visible mould growth. Therefore, we are interested in having a good prediction at lower values for the mould index, where the prediction is reasonably good.
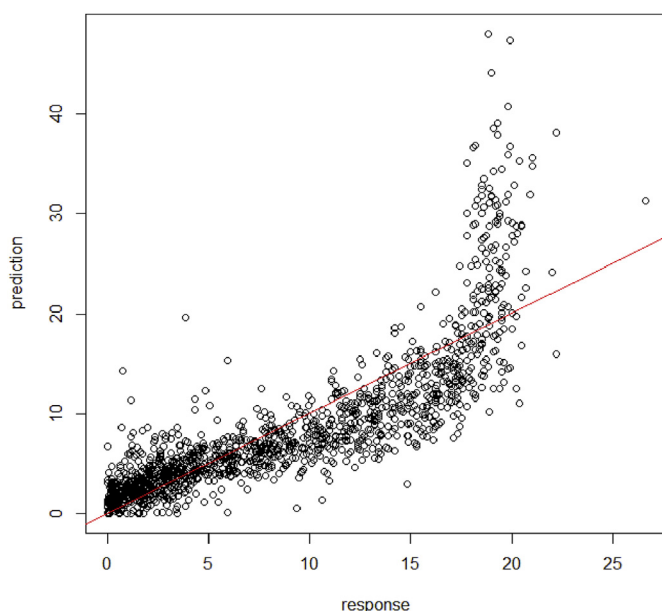

Fig. 5. Comparison of response variable and prediction, for the response variable mould index.

4.4. Prediction

To show the intended use of the developed method, the maximum relative humidity was predicted for various possible scenarios.

In this paper, two input variables were set to describe the analysed wall: orientation γ and short-wave absorption coefficient α_{sw} describe the orientation and the colour of the external surface of the wall; this means that the developed models can be used to assess the moisture risk for the whole range of orientation and colour of the external surface.

Other input variables represent design options that can be evaluated during a moisture risk assessment; in this example the design variables are insulation thickness x_i and rain exposure coefficient k_{rain}. It is therefore possible to assess moisture risk at different levels of insulation thickness, but also to consider the influence of design interventions that can reduce rainwater penetration (e.g. external render, hydrophobic impregnation). The remaining input variables varied according to the distributions identified for the Monte Carlo analysis.

Fig. 6 shows the predicted maximum relative humidity for six possible scenarios. The scenarios represent walls with south-west or north-east orientation, different thickness of woodfibre insulation, x_i, with two levels of rain exposure coefficient ($k_{rain} = 0.7$ and $k_{rain} = 0.3$ [18]). In all scenarios, the short-wave absorption coefficient was $\alpha_{sw} = 0.9$, representing dark red surfaces.

The south-west orientation coincides with the prevailing wind direction and high direct solar radiation; a north-east oriented wall is still subject to some wind-driven rain but receives a very limited amount of direct solar radiation.

The data shown in Fig. 6 are the results of a probabilistic analysis performed with the first of the statistical meta-models presented in this paper, considering maximum relative humidity as response variable. For each scenario, a distribution of maximum relative humidity was found by performing a prediction with the developed statistical meta-model. Scenario 1 shows that, for a wall with 120 mm of woodfibre insulation, the maximum relative humidity is higher for the south-west orientation than for the north-east orientation. Scenario 2 shows the results for a thinner layer of woodfibre insulation, where the maximum relative humidity is higher for the north-east orientation.

Scenarios 3 and 4 represent the same walls with lower exposure to rain, provided by interventions that can reduce rainwater absorption of a surface; a 40% reduction of rain exposure leads to a considerable reduction of maximum relative humidity for the north-east orientation with an insulation thickness of 120 mm, some reduction in the south-west wall and no change in the north-east wall with 40 mm insulation. Comparing the insulation thicknesses, a thinner insulation leads to an increase of maximum relative humidity for the wall with north-east orientation and a decrease of maximum relative humidity for the south-west orientation.

In practical terms, if the moisture risk assessment considered 95% maximum relative humidity as failure criterion, the assessment suggests that a 120 mm-thick woodfibre insulation is preferred to a thinner insulation for the north-east wall. The risk can be further reduced with interventions that reduce the surface rainwater absorption. This suggests that indoor and outdoor moisture sources play a similar role in the moisture balance of a north-east wall for the location assessed; a moderate rainwater absorption reduces the influence of external moisture sources and a thicker insulation leads to a slightly higher vapour resistance of the system, reducing vapour accumulation from indoor sources.

The moisture risk assessment for the south-west wall suggests that a 40 mm-thick insulation leads to lower moisture risk than thicker insulation, combined with interventions to reduce the surface rainwater absorption; however, the influence of insulation thickness on the moisture risk is lower than at the previous orientation. This suggests that outdoor moisture sources might have a higher influence on the moisture risk than indoor sources. Also, it is important to note that the location selected for the analysis is one of the most extreme wind-driven
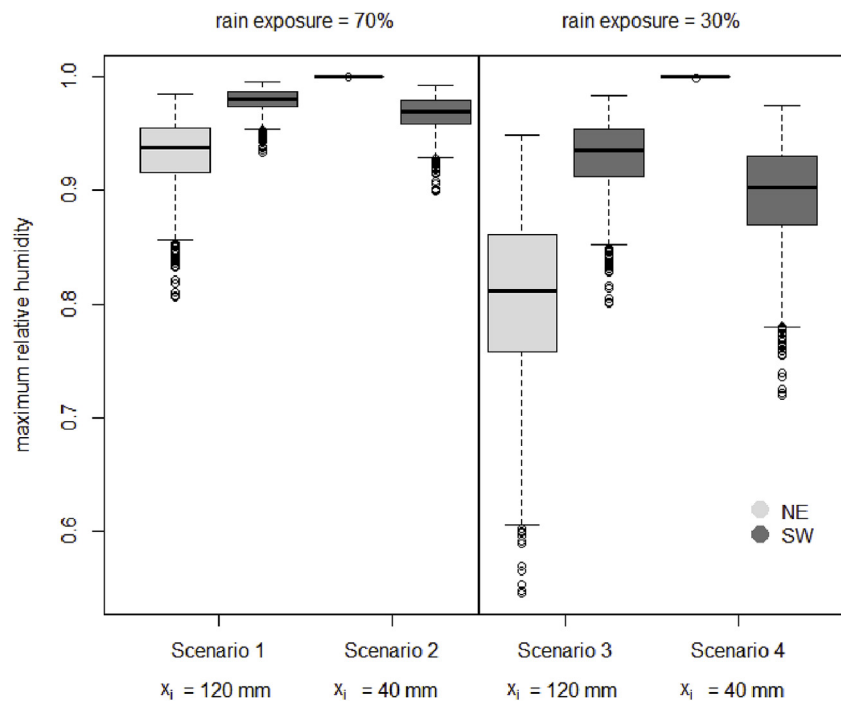
Fig. 6. Comparison of scenarios, for the response variable maximum relative humidity.

rain exposure areas in the UK [64]. This location was selected to show the influence of orientation on moisture risk. However, in areas with extremely high exposure to wind-driven rain, one can find external surface materials that allow low water absorption, such as slate or tiles [65].

Other studies have identified and confirmed the influence of rain exposure on the moisture risk of internally insulated solid walls, in areas exposed to wind-driven rain [14,15,18,66]; some authors have also concluded that under moderate rain, the performance of capillary active systems is satisfactory [14,18]. Moreover, studies have confirmed that the insulation thickness, which affects the vapour diffusion resistance of insulation, can have a significant influence on the hygrothermal performance of a wall insulated with a capillary active system [26].

5. Conclusion

This paper presents an approach to build statistical models for the probabilistic risk assessment of moisture accumulation, when solid wall buildings are insulated. The risks related to moisture accumulation at the interface between existing wall and insulation were assessed. Various criteria can be considered for the analysis, including percentage-based criteria (e.g. maximum relative humidity) and dose-response criteria (e.g. mould index).

The process included a Monte Carlo analysis for obtaining the response variables, a sensitivity analysis to identify non-influential input variables (with respect to the response variable), followed by the construction of two statistical models, one for the prediction of maximum relative humidity and another for the prediction of the mould index.

It was found that both risk assessment models had a good predictive power, hence highlighting the advantages of using GAM and GAMLSS. The models can be improved considering interactions among covariates in which case bigger sample sizes would have to be considered.

Following the proposed method, it is possible to build predictive models considering different wall thickness, types of masonry and insulation.

These predictive models can be developed to be used by professionals for a fast moisture risk assessment of solid walls when subject to internal insulation retrofit. They can replace computationally intensive simulations and provide additional information related to the spread of the response variable in a few seconds. Multiple criteria can be used simultaneously in the process of risk assessment; further work will explore the use of predictive models to allow for this. This process, now confined to one location, can be extended to consider a regional area, or more.

Declarations of interest

None.

Acknowledgements

References

[1] Committee on Climate Change, (June), 2017 Report to Parliament Meeting Carbon Budgets: Closing the Policy Gap vol. 203, (2017).

[2] British Research Establishment, Energy Analysis Focus Report a Study of Hard to Treat Homes Using the English House Condition Survey, Technical report (2008).

[3] HM Department for Communities and Local Government, Technical Report, English Housing Survey. Headline Report vol. 8010, (2017).

[4] Masaru Abuku, Hans Janssen, Staf Roels, Impact of wind-driven rain on historic brick wall buildings in a moderately cold and humid climate: numerical analyses of mould growth risk, indoor climate and energy consumption, Energy Build. 41 (1) (jan 2009) 101–110.

[5] Chryso Heracleous, Ioannis Ioannou, Maria Philokyprou, Aimilios Michael, Hydrothermal performance of a stone masonry wall in a traditional building in Cyprus, Edinburgh, PLEA 2017-Design to Thrive, 2017, pp. 5030–5037.

[6] Evy Vereecken, Liesje Van Gelder, Hans Janssen, Staf Roels, Interior insulation for wall retrofitting A probabilistic analysis of energy savings and hygrothermal risks, Energy Build. 89 (2015) 231–244.

[7] Dominique Derome, Jan Carmeliet, The Nature, Significance and Control of Solar-driven Water Vapor Diffusion in Wall Systems Synthesis of Research Project RP-1235 vol. 116, (2010).

[8] Valentina Marincioni, Hector Altamirano-Medina, Effect of orientation on the hygrothermal behaviour of a capillary active internal wall insulation system, 10th Nordic Symposium on Building Physics, 2014, pp. 1238–1243.

[9] Akram Abdul Hamid and Petter Wallentén, Hygrothermal assessment of internally added thermal insulation on external brick walls in Swedish multifamily buildings, Build. Environ. 123 (2017) 351–362.

[10] Dominique Derome, Saba Saneinejad, Inward vapor diffusion due to high temperature gradients in experimentally tested large-scale wall assemblies, Build. Environ. 45 (12) (dec 2010) 2790–2797.

[11] BSI. BS EN 15026:2007, Hygrothermal Performance of Building Components and Building Elements Assessment of Moisture Transfer by Numerical Simulation, (2007).

[12] Hartwig M. Künzel, Effect of interior and exterior insulation on the hygrothermal behaviour of exposed walls, Mater. Struct. 31 (2) (mar 1998) 99–103.

[13] Daniel Kehl, Ulrich Ruisinger, Rudolf Plagge, John Grunewald, Holzbalkenköpfe bei innengedämmten Mauerwerk Ursachen der Holzzerstörung und Beurteilung von Holz zerstörenden Pilzen, 2. Internationaler Innendämmkongress, 2013.

[14] E. Vereecken, S. Roels, Capillary active interior insulation: do the advantages really offset potential disadvantages? Mater. Struct. 48 (9) (2014) 3009–3021 http://doi.org/10.1617/s11527-014-0373-9.

[15] P. Häupl, J. Grunewald, U. Ruisinger, Hygrothermal analysis of external walls within the reconstruction of the Rijksmuseum Amsterdam, Structural Studies, Repairs and Maintentance of Heritage Architecture IX, vol. 83, WIT Press, 2005, pp. 345–354.

[16] M. Guizzardi, J. Carmeliet, D. Derome, Risk analysis of biodeterioration of wooden beams embedded in internally insulated masonry walls, Construct. Build. Mater. 99 (2015) 159–168.

[17] M. Harrestrup, S. Svendsen, Internal insulation applied in heritage multi-storey buildings with wooden beams embedded in solid masonry brick façades, Build. Environ. 99 (2016) 59–72.

[18] Jianhua Zhao, John Grunewald, Ulrich Ruisinger, Shuo Feng, Evaluation of capillary-active mineral insulation systems for interior retrofit solution, Build. Environ. 115 (2017) 215–227.

[19] Anton Tenwolde, ASHRAE Standard 160P _ criteria for moisture control design analysis in buildings, Build. Eng. (2008) 167–172.

[20] Hartwig Kunzel, Accounting for unintended moisture sources in hygrothermal building analysis, Lund, Proceedings of the 10th Nordic Symposyum of Building Physics, 2014, pp. 947–953.

[21] Gholam Reza Finken, Søren Peter Bjarløv, Ruut Hannele Peuhkuri, Effect of façade impregnation on feasibility of capillary active thermal internal insulation for a historic dormitory - a hygrothermal simulation study, Construct. Build. Mater. 113 (2016) 202–214.

[22] U.S. Environmental Protection Agency, Risk Assessment Forum White Paper: Probabilistic Risk Assessment Methods and Case Studies, EPA/100/R-14/004. (July), vol. 98, (2014).

[23] S. Ratick, G. Schwarz, Monte Carlo simulation, Int. Encycl. Hum. Geogr. (2009) 175–184.

[24] Jianhua Zhao, Rudolf Plagge, John Grunewald, Performance assessment of interior insulations by a stochastic method, 9th Nordic Symposium on Building Physics NSB2011, vol. 1, 2011, pp. 465–472.

[25] Endrik Arumägi, Margus Pihlak, Targo Kalamees, Reliability of interior thermal insulation as a retrofit measure in historic wooden apartment buildings in cold climate, Energy Procedia 78 (2015) 871–876.

[26] Astrid Tijskens, Hans Janssen, Staf Roels, Retrofitting historical buildings: a probabilistic assessment of interior insulation measures and the hygrothermal risks, 4th WTA International PhD Symposium, 2017, pp. 149–156 Delft.

[27] Klodian Gradeci, Nathalie Labonnote, Berit Time, Jochen Köhler, A probabilistic-based methodology for predicting mould growth in façade constructions, Build. Environ. 128 (October 2017) 33–45 2018.

[28] Carl Eric Hagentoft, Reliability of energy efficient building retrofitting - probability assessment of performance and cost (Annex 55, RAP-RETRO), Energy Build. 155 (2017) 166–171.

[29] Krystyna Pietrzyk, A Systemic Approach to Moisture Problems in Buildings for Mould Safety Modelling vol. 86, (2015), pp. 50–60.

[30] Hans Janssen, Staf Roels, Liesje Van Gelder, Payel Das, Annex 55, Subtask 2 Probabilistic Tools, Technical report (2014).

[31] Liesje Van Gelder, Payel Das, Hans Janssen, Staf Roels, Comparative study of metamodelling techniques in building energy simulation : guidelines for practitioners, Simulat. Model. Pract. Theor. 49 (2014) 245–257.

[32] Wei Tian, A review of sensitivity analysis methods in building energy analysis, Renew. Sustain. Energy Rev. 20 (2013) 411–419.

[33] Evy Vereecken, Staf Roels, Hygric performance of a massive masonry wall: how do the mortar joints influence the moisture flux? Construct. Build. Mater. 41 (apr 2013) 697–707.

[34] Francis G.N. Li, A.Z.P. Smith, Phillip Biddulph, Ian G. Hamilton, Robert Lowe, Anna Mavrogianni, Eleni Oikonomou, Rokia Raslan, Samuel Stamp, Andrew Stone, A.J. Summerfield, David Veitch, Virginia Gori, Tadj Oreszczyn, Solid-wall U-values: heat flux measurements compared with standard assumptions, Build. Res. Inf. 43 (2) (2014) 238–252, http://dx.doi.org/10.1080/09613218.2014.967977.

[35] Jianhua Zhao, Rudolf Plagge, Nuno M.M. Ramos, M. Lurdes Simões, John Grunewald, Concept for development of stochastic databases for building performance simulation A material database pilot project, Build. Environ. 84 (2015) 189–203.

[36] J. Zhao, R. Plagge, N.M. Ramos, M.L. Simoes, J. Grunewald, Application of clustering technique for definition of generic objects in a material database, J. Build. Phys. 39 (2) (2015) 124–146.

[37] Andreas Nicolai, John Grunewald, Delphin 5-User Maunal and Program Reference, (2006).

[38] Christopher Hall, Andrea Hamilton, Porosity-density relations in stone and brick materials, Mater. Struct. 48 (5) (2013) 1265–1271.

[39] W.J. Conover, Ronald L. Iman, Rank Transformations as a Bridge between Parametric and Nonparametric Statistics vol. 35, (1981), pp. 124–129 3.

[40] Jianhua Zhao, Development of a Novel Statistical Method and Procedure for Material Characterization and a Probabilistic Approach to Assessing the Hygrothermal Performance of Building Enclosure Assemblies, (2012).

[41] Qiao Ge, Monica Menendez, Extending Morris method for qualitative global sensitivity analysis of models with dependent inputs, Reliab. Eng. Syst. Saf. 162 (2017) 28–39.

[42] Valentina Marincioni, Hector Altamirano-Medina, Identifying a suitable climate file for the moisture risk assessment of internally insulated walls exposed to solar-driven vapour diffusion, Building Simulation 2017, 2017, pp. 2123–2128 San Francisco.

[43] Met Office, Met Office Integrated Data Archive System (MIDAS) Land and Marine Surface Stations Data (1853-current), (2012).

[44] BSI. BS EN ISO 6946, Building Components and Building Elements Thermal Resistance and Thermal Transmittance Calculation Method, Technical report (2007).

[45] Simone Kotthaus, Thomas E.L. Smith, Martin J. Wooster, C.S.B. Grimmond, Derivation of an urban materials spectral library through emittance and reflectance spectroscopy, ISPRS J. Photogrammetry Remote Sens. 94 (2014) 194–212.

[46] I. Ridley, M. Davies, Sh Hong, T. Oreszczyn, Vapour Pressure Excess in Living Rooms and Bedrooms of English Dwellings: Analysis of the Warm Front Dataset, Internal report, IEA-EXCO energy conservation in buildings and community systems program, Annex 41, whole building heat, air and moisture response (MOIST-ENG). In: Seventh Working Meeting, Florianopolis, 16–18 April (2007).

[47] BSI. BS EN ISO 13788, Hygrothermal Performance of Building Components and Building Elements Internal Surface Temperature to Avoid Critical Surface Humidity and Interstitial Condensation Calculation Methods, 2012, (2012).

[48] P.W.M.H. Steskens, H. Janssen, C. Rode, Influence of the convective surface transfer coefficients on the heat, air, and moisture (HAM) building performance, Indoor Built Environ. 18 (3) (jun 2009) 245–256.

[49] Hans Janssen, Monte-Carlo based uncertainty analysis: sampling efficiency and sampling convergence, Reliab. Eng. Syst. Saf. 109 (2013) 123–132.

[50] W.T.A. WTA-Guideline 6-2, Simulation wärme- und feuchtetechnischer Prozesse, (2013).

[51] Jagjit Singh, Building Mycology. Management of Decay and Health in Buildings, E & FN Spon, 1994.

[52] Hannu A. Viitanen, Modelling the time factor in the development of mould fungi - the effect of critical humidity and temperature conditions on pine and spruce sapwood, Holzforschung 51 (1) (1997) 6–14.

[53] Tord Isaksson, Sven Thelandersson, Annika Ekstrand-Tobin, Pernilla Johansson, Critical conditions for onset of mould growth under varying climate conditions, Build. Environ. 45 (7) (2010) 1712–1721.

[54] Max D. Morris, Factorial sampling plans for preliminary computational experiments, Technometrics 33 (2) (1991) 161.

[55] Francesca Campolongo, Andrea Saltelli, Jessica Cariboni, From screening to quantitative sensitivity analysis. A unified approach, Comput. Phys. Commun. 182 (4) (2011) 978–988.

[56] Simon N. Wood, Generalized Additive Models: an Introduction with R, second ed., CRC Press, 2017.

[57] R.A. Rigby, D.M. Stasinopoulos, Generalized additive models for location, scale and shape, Appl. Stat. 54 (2005) 507–554.

[58] Giampiero Marra, Rosalba Radice, Bivariate copula additive models for location, scale and shape, Comput. Stat. Data Anal. 112 (2017) 99–113.

[59] H. Viitanen, A. Ritschkoff, Mould Growth in Pine and Spruce Sapwood in Relation to Air Humidity and Temperature, Technical report, Swedish University of Agricultural Sciences, Department of Forest Products, Uppsala, 1991.

[60] A. Hukka, Hannu Viitanen, A mathematical model of mould growth on wooden material, Wood Sci. Technol. 33 (1999) 475–485.

[61] Tuomo Ojanen, Hannu Viitanen, Ruut Peuhkuri, Juha Vinha, Kati Salminen, Mold Growth Modeling of Building Structures Using Sensitivity Classes of Materials, (2010).

[62] Hannu Viitanen, Tuomo Ojanen, Improved model to predict mold growth in building materials, Thermal Performance of the Exterior Envelopes of Whole Buildings X, 2007 Clearwater Beach, USA.

[63] H. Viitanen, M. Krus, T. Ojanen, V. Eitner, D. Zirkelbach, Mold risk classification based on comparative evaluation of two established growth models, Energy Procedia 78 (2015) 1425–1430.

[64] C. Stirling, BR 262 Thermal Insulation: Avoiding Risks, third ed., BRE Press, 2002.

[65] Peter Trotman, Chris Sanders, Harry Harrison, Understanding Dampness. Effects, Causes, Diagnosis and Remedies, Technical report, BRE (2004).

[66] Timo De Mets, Antoine Tilmans, Xavier Loncour, Hygrothermal assessment of internal insulation systems of brick walls through numerical simulation and full-scale laboratory testing, Energy Procedia 132 (2017) 753–758.

[67] S.N. Wood, mgcv: Mixed GAM Computation Vehicle with Automatic Smoothness Estimation, (2018) R package version 1.8-23. URL http://CRAN.R-project.org/package=mgcv.

[68] G. Marra, R. Radice, GJRM: Generalised Joint Regression Modelling, R package version 0.1-4. URL, 2018. http://CRAN.R-project.org/package=GJRM, .